9th International Conference on Structural Health Monitoring of Intelligent Infrastructure
2019 ST. LOUIS SHMII-9
AUGUST 4-7, 2019 | St. Louis, Missouri USA
Organized by MISSOURI S&T

Considerations for Hose Wielding UAV for Civil Infrastructure Cleaning

Blake Hament[1], Paul Oh [2]
[1] *Mechanical Engineering Department, University of Nevada, Las Vegas – USA,*
Email: blake.hament@unlv.edu
[2] *Mechanical Engineering Department, University of Nevada, Las Vegas – USA,*

Abstract

To expand the capabilities of a multi-rotor aerial vehicle, one or several hoses could be mounted to the vehicle. Such hoses could be used to expel compressed air or other fluid for the purpose of cleaning hard-to-reach surfaces. The main challenge in operating a hose mounted on a free-flying aerial vehicle is compensating for the reaction forces and torques the vehicle experiences as fluid leaves the hose. This paper introduces dynamic modeling for a hose mounted on a multi- rotor vehicle. It is shown that safe operating ranges can be defined in terms of hose angle and fluid PSI, with instability occurring outside of this bounded tool-space. Insights from model analysis are presented to help the reader apply key takeaways to vehicle and controller design.

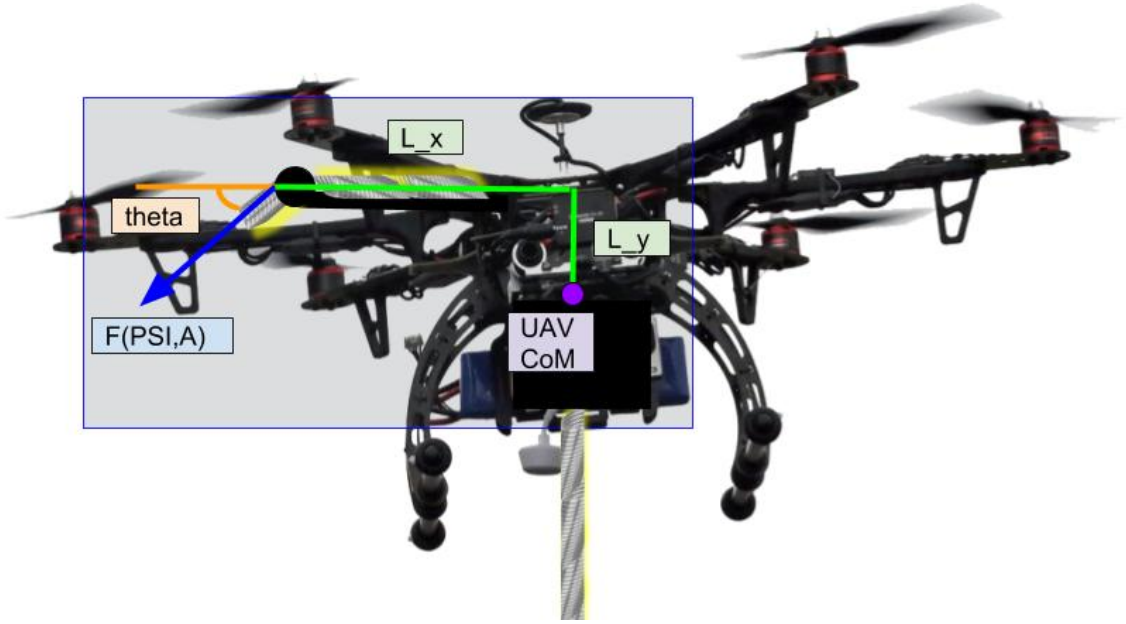

Figure 1. A hose is mounted on a multi-rotor UAV such that it remains in a plane perpendicular to the ground and containing UAV center of mass.

1. Introduction

According to the American Society of Civil Engineers, US infrastructure has consistently scored a "D" average over the last three decades (ASCE 2016). With so many bridges and overpasses in critical condition, the US Department of Transportation would benefit significantly from

increased efficiency in inspection and repair. To optimize time and resources for repair – regular, high-resolution inspection data should be collected. Traditionally this infrastructure inspection has been performed by small manned teams that travel to inspection sites. Often the infrastructure on site must be cleaned before high- resolution inspection data can be captured. Human inspectors are suspended from cherry-pickers or other specialized crane vehicles while they spray the infrastructure with pressurized air, water, or some chemical cleaning mixture. This procedure is dangerous, time-consuming, and strenuous. Instead, a multi-rotor vehicle could be equipped with a hose to perform this cleaning task. With an on-board camera and other non-destructive evaluation (NDE) sensors, the vehicle could collect inspection data immediately after cleaning, decreasing overall site time and further eliminating risks for human inspectors.
The rest of the paper is organized as follows: Section II reviews relevant literature; Section III derives an analytic model for hose-vehicle system dynamics; Section IV discusses important results from the analytic model; and Section V concludes.

2. Literature Review

Important progress has already been made towards realizing robotic systems for automated civil infrastructure inspection and repair. A team led by roboticists at Rutgers University demonstrated the RABIT robot, a ground vehicle equipped with NDE sensors like impact echo, electrical resistivity, and ground-penetrating radar devices (La 2013). RABIT can move itself across a bridge or overpass, navigating using GPS data and collecting NDE data on the structure below.

While RABIT is an essential and valuable contribution that demonstrates successful integration NDE sensors on an autonomous robot, it still requires lane closures to operate. In comparison, an unmanned aerial vehicle (UAV) could hover above a bridge or overpass and collect data without requiring dangerous lane closures that disrupt the normal flow of traffic. The Aerial Robotic Infrastructure Analyst (ARIA) project from Carnegie Melon University follows this approach (ARIA 2015). The team has developed navigation, flight control, and LiDAR data capture and processing software for multi-rotor UAV, such that an aerial vehicle can autonomously perform bridge inspection from the air. Stitching together the multi-modal data captured from varying aerial perspectives is no small task, and this remains an active area of research (Lacroix 2010).
An important challenge and research gap remains for applying multi-rotor UAV to civil infrastructure inspection. Over the course of their lifetime, large pieces of civil infrastructure often collect layers of dust and other small particulates. These layers of particles obscure visual inspection, often hiding significant indicators of bridge health or defects. It is current practice to equip human inspectors with a hose that sprays compressed air or water and to send them up on ladders or cherry-pickers to clean the infrastructure surfaces before visual inspection. Of course, this places human inspectors in a precarious position with increased risk of fall from the backwash of fluid and dislodged particles. To keep human inspectors out of harm's way, aerial inspection vehicles should be developed such that they can operate a hose and clean infrastructure before beginning visual scanning.

3. Derivation of Analytic Model

3.1 Hose Force

The force F_H exerted on a UAV from fluid with density ρ being expelled at velocity v through a hose with area A is modeled as

$$F_H = v\,\frac{dM}{dt} = v(\rho A v) = \rho A v^2 = pA\,. \tag{1}$$

Pressure loss from ground compressor to hose nozzle can be modeled with the Darcy Equation and some additional physical characteristics of the hose: length L, diameter D; and friction factor f_D obtained experimentally. Assuming incompressible flow with velocity v, pressure loss is

$$\Delta p = f_D \frac{L}{D}\frac{\rho v^2}{2}\,. \tag{2}$$

Thus the force from fluid compressed to p_0 then expelled from a hose with the above characteristics is

$$F_H = \left(p_0 - f_D \frac{L}{D}\frac{\rho v^2}{2}\right) A\,. \tag{3}$$

3.2 Generalized Force and Torque

Consider a hose mounted to a UAV as shown in Fig. 1. The hose is mounted such that it passes through the vehicle's center of mass (CoM) and remains coplanar with this point as it snakes along the frame to the nozzle mount. Within the shared plane, the nozzle is mounted at some horizontal offset L_X and some vertical offset Ly from the CoM. The nozzle points at some angle θ_n below the horizon, still coplanar with the CoM. This angle depends on the angle from the frame to the nozzle θ_0 and the current pitch of the vehicle θ,

$$\theta_n = \theta_0 + \theta \tag{4}$$

The generalized x and y components of force and perpendicular torque is thus

$$\begin{bmatrix} F_{Hx} \\ F_{Hy} \\ \tau_H \end{bmatrix} = \begin{bmatrix} F_H \cos\theta_n \\ -F_H \sin\theta_n \\ L_y F_H \cos\theta_n + L_x F_H \sin\theta_n \end{bmatrix} \tag{5}$$

3.2 Vehicle Characteristics

In general, we expect from Newton's 3rd Law that vehicles with lower mass and inertia will be accelerated more than UAV with high inertia under the same hose force,

$$\begin{bmatrix} \sum F_x \\ \sum F_y \\ \sum \tau \end{bmatrix} = \begin{bmatrix} M\,\ddot{x} \\ M\,\ddot{\theta} \\ I_z \ddot{\theta} \end{bmatrix}. \tag{6}$$

The UAV's total available thrust plays an important role in how much hose force can be compensated before actuator saturation occurs and such accelerations are experienced. Given a multi-rotor UAV with an even number n rotors and thrust u_i from each motor mounted at

horizontal offset Lx_i from CoM, the generalized x and y components of force and perpendicular torque from the rotors is

$$\begin{bmatrix} F_{Ux} \\ F_{Uy} \\ \tau_{Uz} \end{bmatrix} = \begin{bmatrix} \sum u_i \cos\theta_n \\ \sum u_i \sin\theta_n \\ \sum L_x u_i \end{bmatrix}. \quad (7)$$

For the case that the UAV is constrained to the hose-CoM plane, equation 7 can be approximated with a total thrust left and total thrust right of CoM, U_L and U_R respectively, and averaged horizontal motor mount CoM offsets L_{ax}:

$$\begin{bmatrix} F_{Ux} \\ F_{Uy} \\ \tau_{Uz} \end{bmatrix} \approx \begin{bmatrix} (U_L + U_R)\cos\theta_n \\ (U_L + U_R)\sin\theta_n \\ L_{ax}(U_L - U_R) \end{bmatrix}. \quad (8)$$

In equation 8, the n control voltages that create thrusts u_i are simplified to just two control inputs u_L and u_R to probe the limits of UAV controllability with respect to hose forces and torques, just in the hose-vehicle plane, such that

$$U_L = \frac{n}{2}u_L \text{ and } U_R = \frac{n}{2}u_R \, . \quad (9)$$

3.2 Combined Hose-Vehicle Dynamics

To regulate position of a UAV while operating a hose mounted as discussed above, the forces and torque generated by rotor thrust should cancel those of the hose, such that

$$\begin{bmatrix} \sum F_x \\ \sum F_y \\ \sum \tau_z \end{bmatrix} = \begin{bmatrix} 0 \\ 0 \\ 0 \end{bmatrix} = \begin{bmatrix} F_{Hx} + F_{Ux} \\ -F_{Hy} + F_{Uy} - Mg \\ \tau_H + \tau_{Uz} \end{bmatrix}. \quad (10)$$

4. Results & Discussion

4.1 Stable Tool-space

From the above modeling, we can begin to quantify bounds on system stability. Assume hose operation begins with low compression pressure, while the vehicle is in stable hover, and is gradually increased to desired operating value. If the UAV is to hold position and operate hose from its initial pose, then the bounds on operation are obtained from solving equation 10 and analyzing constraints.

In initial hardware tests, it was quite clear that the size of the multi-rotor UAV greatly influenced its stability while operating a hose. To probe theory for this type of behavior, equation 10 was evaluated for 3 distinct vehicle configurations. The vehicle configurations were selected to represent archetypal small, medium, and large UAV available today. Table 1 provides more detail on the vehicle masses, frame lengths, and number of rotors. For each vehicle, the tool-space is interrogated with respect to stability along each degree of freedom.

It is useful and interesting to examine decoupled solutions to equation 10. Figures 2, 3, and 4 are presented to illustrate hard limits on hose operation. In the 3D surface plots, the ground plane is the tool-space, comprised by permutations of hose pressure and angle. Above the tool-space plane, the surface values represent necessary thrust to maintain position hold. This thrust is color-coded by percentage of total thrust available to the vehicle. Safe operation is denoted by blue and green shading. Possible but risky operation is shaded yellow at 70 % full throttle, orange at 80 %, and light red at 90 %. Theory predicts uncontrollability and instability for any part of the tool-space with dark red shading overhead, as this would require more than 100 % throttle to compensate for hose reaction forces and torques.

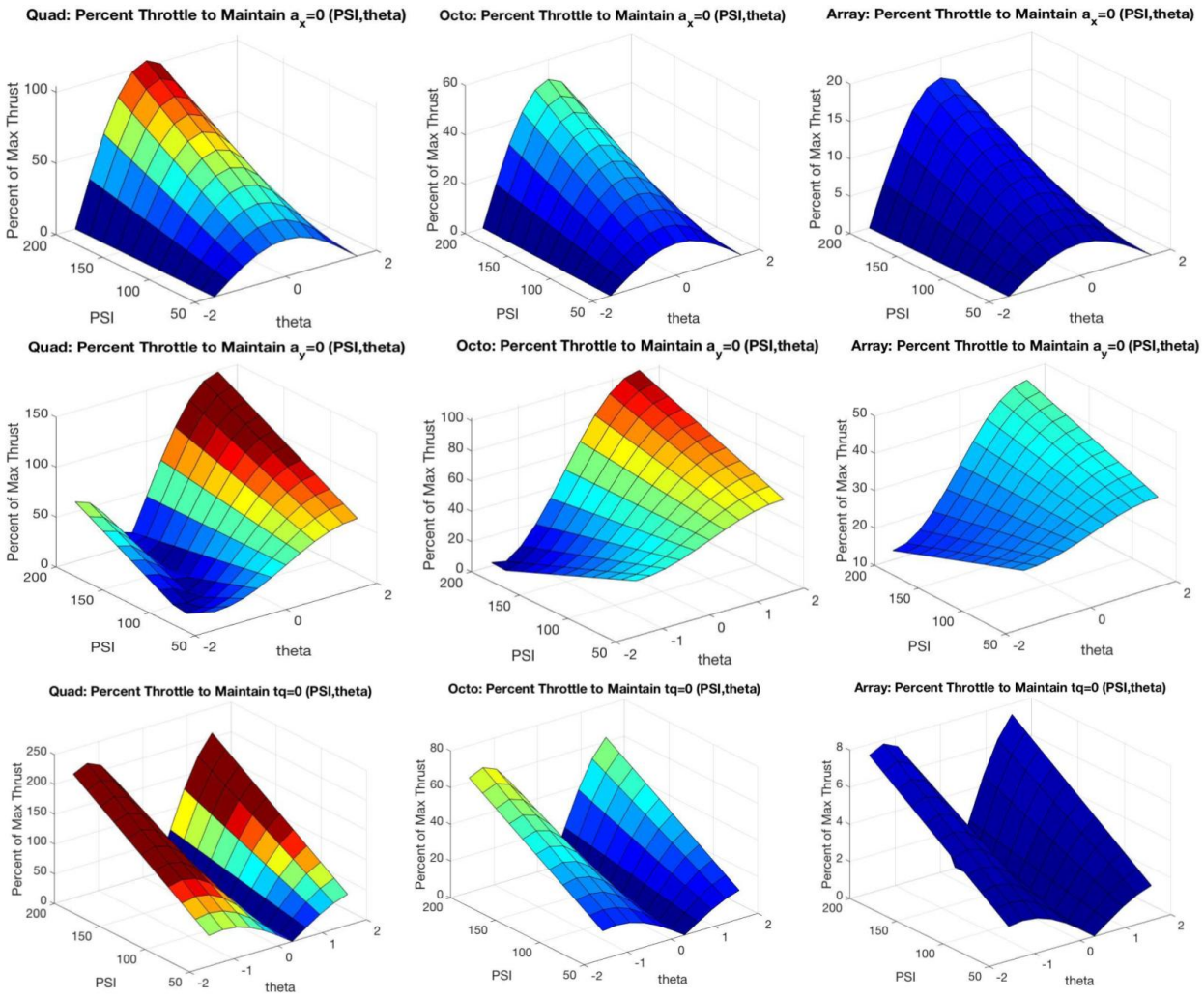

Figure 2. Safe tool-space limits for maintaining zero acceleration are illustrated for quadcopter (A), octocopter (B), and array copter (C) by column respectively. First row of surface plots shows limits from maintaining zero horizontal acceleration. Second row of plots shows limits from zero vertical acceleration constraint. Last row visualizes limits from zero angular acceleration.

4.2 Takeaways for Vehicle and Controller Design

It is clear from figures 2, 3, and 4 that the larger the vehicle, the larger the available safe tool-space. This is quite intuitive when considering that larger vehicles have more inertia, such that

they are less affected by a given hose force and torque than smaller vehicles. Additionally, the larger vehicles have more rotors with which to compensate for hose reaction forces and torques, such that they can counteract the hose at lower percentages of full throttle thrust.

Nonetheless, Figure 4 demonstrates that even with a small UAV, it is possible to safely operate with very high hose pressures if the hose is mounted strategically. For a given hose pressure and angle, UAV designers can adapt hose mounting offsets Lx and Ly to adjust the reaction torque produced by hose. UAV controller designers working with a given UAV frame and hose mounting configuration can adjust hose angle θ and UAV pose in space to safely access high pressures according to equation 10.

Table 1.

Vehicle:	**Quad (A)**	**Octo (B)**	**Array (C)**
Mass (kg)	5	15	60
Rotors (n)	4	8	24
Arm Length Mean (m)	.15	.25	.5

5. Conclusion

This paper presents modeling and simulated results to aid multi-rotor designers and operators to develop UAV to operate a hose that expels compressed air or water. Force and torque due to hose are modeled and incorporated into a system of equations governing dynamics of the hose-UAV system. From this system of equations, limits on hose pressure and angle are developed for safe operation. Safe tool-space is visualized with color-coding to help designers and pilots to choose hose pressure and angle appropriate for their respective UAV. UAV with more inertia and rotors can access more extreme hose pressures and angles than smaller vehicles.

References

ARIA Team (2015). “The Aerial Robotic Infrastructure Analyst (ARIA) project.” http://aria.ri.cmu.edu/.

ASCE. “Failure to Act: The Impact of Infrastructure Investment on Amer- ica’s Economic Future”, American Society of Civil Engineers Reston Virginia, 2016.

H. La, R. Lim, B. Basily, N. Gucunski, J. Yi, A. Maher, F. Romeroand H. Parvardeh, “Autonomous robotic system for high-efficiency non- destructive bridge deck inspection and evaluation”, IEEE International Conference on Automation Science and Engineering (CASE), 2013.

S. Lacroix and G. Le Besnerais, “Issues in Cooperative Air/Ground Robotic Systems”, Springer Tracts in Advanced Robotics, pp. 421-432, 2010.